Journal of Visualization, Vol. 7, No. 4 (2004) 341-348

An investigation on airflow in pathological nasal airway by PIV

Kim, S. K.[*1] and Haw, J. R.[*2]

*1 Dept. Mechanical Eng., Konkuk University, 1 Hwayang-dong Kwanggin-ku Seoul, 143-701, Korea.
E-mail: sungkim@kkucc.konkuk.ac.kr
*2 Dept. Materials Chem.& Eng., Konkuk University, 1 Hwayang-dong Kwanggin-ku Seoul, 143-701, Korea.

Received 18 July 2003
Revised 15 April 2004

Abstract : Understanding of airflow characteristics in nasal cavity is closely related with the physiological functions, like air-conditioning and smelling, and pathological aspects in nasal breathing. Several studies have utilized physical models of the healthy nasal cavity to investigate the relationship between nasal anatomy and airflow. The next step on this topic is naturally studies for disordered nasal airways and this is the main purpose of this article. Airflows in the pathological nasal airways, including nasal cavity and upper pharynx, of Korean adults are investigated experimentally by PIV measurement technique and air resistance measurements. Quantitative data for normal and pathological nasal airway are obtained. Average and RMS velocity distributions are obtained for inspirational and expirational nasal airflows. The CBC PIV algorithm with window offset is used for PIV flow analysis. PIV measurements of nasal airflow for nasal cavities with 50% and 70% adenoid vegetation are conducted for the first time. The asymmetric nasal cavities, due to either congenital deformity or injury, are also investigated. Comparisons in nasal airflows for both normal and abnormal cases are also appreciated and airflow characteristics that are related with the abnormalities in nasal cavity are proposed.

Keywords : Bio-Fluid Flow, Nasal Air Flow, PIV, CT (Computed Tomogram), Adenoid Vegetation.

1. Introduction

Knowledge of airflow characteristics in nasal cavity is essential to understand the physiological and pathological aspects of nasal breathing. Therefore, many medical and biomechanical researches have investigated on nasal airflow. Several studies have utilized physical models of the nasal cavity in an effort to understand the relationship between nasal anatomy and the distribution of inspired and expired airflow. Among others, Scherer et al. (1989) measured airflow rate in a large (20 times) model, constructed from computed tomograms (C.T), using a hot-wire anemometer (HWA). Hess et al. (1992) reported flow visualization results of dye-streak photos. Their model was made of clear silicone through casting in a death body. Hopkins et al. (2000) recently established a procedure to construct a transparent rectangular box containing a model of the nasal cavity for PIV measurement by combination of the Rapid Prototyping (RP) and the curing of clear silicone. In authors' previous paper (Kim et al., 2002a), airflows in the normal nasal cavities of Korean are investigated experimentally by PIV measurement. (Kim et al., 2002b)

The next step on this topic is naturally studies for disordered nasal airways and this is the main purpose of this article. Two pathological airway cases, one with Adenoid Vegetation and the asymmetric nasal cavities due to either congenital deformity or injury are investigated by PIV. The CBC PIV algorithm (Hart, 2000) with window offset is used for PIV flow analysis. Creating the

accurate transparent flow passages is essential to analyzing the flow inward a complex flow passage by PIV. With dense CT scan data (166 data with 0.6mm scan thickness) and careful surface rendering, more sophisticated nasal cavity model can be made and used in this article.

Comparison of airflows for a normal and a disordered nasal cavity are appreciated. Adenoid vegetation exceeding 60% causes a rapid increase in pressure drop between nares and nasopharynx. The PIV results confirm this fact through the comparison of flow characteristics and RMS quantities at nasopharynx between models of 50% and 70% adenoid vegetation. One case of an asymmetric nasal cavity due to bent of nasal septum is dealt in this study. Even though the geometries of left and right cavities are quite different, flow rates of both cavities are almost even in this case. This can be explained by the fact that this patient's nose adapts itself to this circumstance by deforming the other parts of nasal cavities.

The paradigm established in this paper can be applied to many kinds of otorhinolaryngological diseases and is believed to contribute to the diagnosis and treatment including medical operation of nasal diseases.

2. Flow passage inside nose and nasal anatomy

A brief nasal anatomy, related with the analysis on nasal airflow, is depicted in Fig. 1. Two nasal cavities are separated by a nasal septum. A nasal airway is mainly composed of three hooked passages (inferior, middle, superior airway) enclosed by nasal septum and inferior, middle, superior conchas: Green colored section in Figs. 1(b, c). In a state of relaxation, one of nasal cavities is used alternately for a period of hours. Most flow rates are believed to pass through the middle and inferior miatuses. Usually, parts of the passage can be blocked or bent by disease or injury. Therefore, having consulted with an otorhinolaryngologist, CT scan data of a Korean adult after modification in computer graphic is adopted as the nasal cavity model.

Among otorhinolaryngological diseases for children, the adenoid vegetation is one of the most frequent, and which causes the breath difficulty. General symptoms are the tendency of mouth breathing caused by a blocked nose, incorrect pronunciation, etc. For a flow passage of a nasal cavity with adenoid vegetation, 50% and 70% in cross-sectional area are removed from a replicate model of normal cavity under an ENT doctor's advice, as shown in Fig. 2. The asymmetric nasal cavities, due to either congenital deformity or injury, are very popular. Sometimes this deformity becomes critical turn, results in the medical surgery. Figure 3 depicts a sample of CT scan data for an asymmetric nasal cavity. Airflows in each cavity are compared.

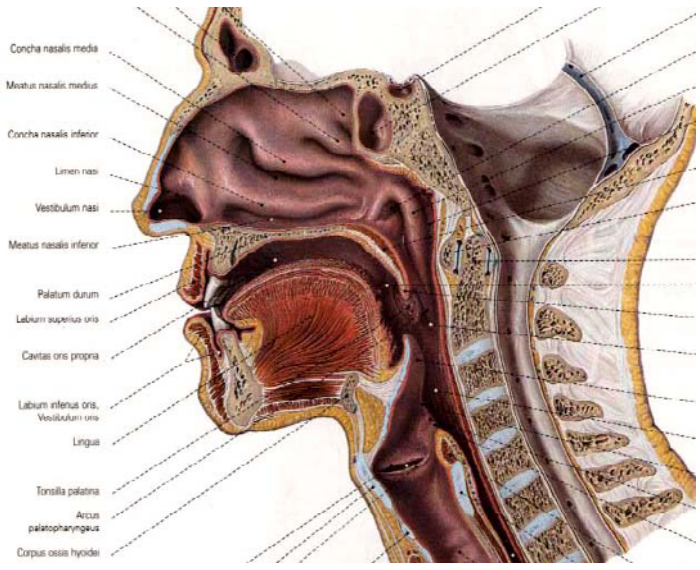

(a) Sagittal view of nasal anatomy (Frick et al., 1990)

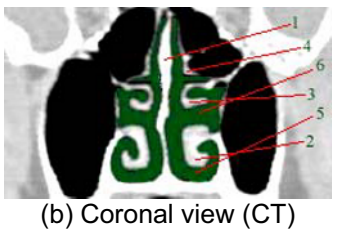

(b) Coronal view (CT)

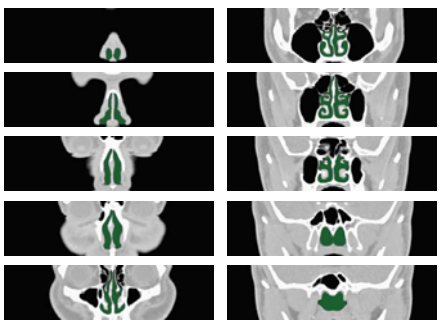

(c) Selected coronal CT scan data

Fig. 1. Nasal anatomy: 1. Nasal septum 2. Inferior concha 3. Middle concha 4. Superior concha 5. Inferior airway 6. Middle airway.

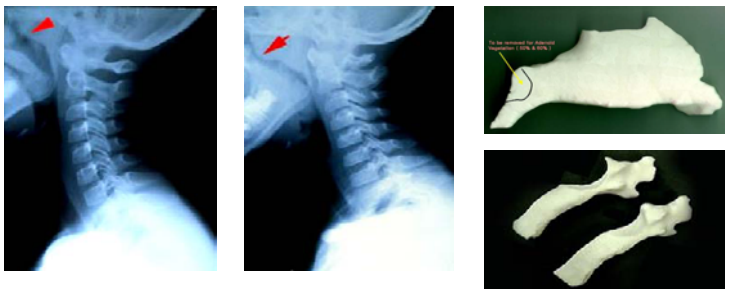

Fig. 2. X-ray photos and models for adenoid vegetation (50% and 70%).

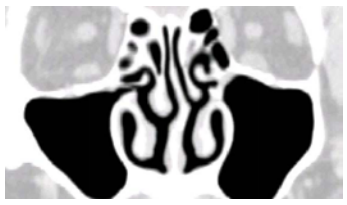

Fig. 3. CT for qsymmetric nasal cavities.

3. Creation of Flow Passage and Experimentation

Creating an accurate transparent flow passages is essential to analyzing the flow inward a complex flow passage by PIV. The key to producing a geometrically complex flow passage suitable for PIV is the recent availability of a rapid prototyping machine (RP) and water-soluble material for a negative model. (Hopkins et al., 2000) Rapid prototyping is a well-accepted method for quickly generating replicate prototypes from computer files including CT scan data. The procedure of creating flow passages is summarized as follows. (Kim et al., 2002a)

1. A solid computer model for building the replicate model is created from dense coronal CT scan data of a healthy Korean adult's nose. (Some selections of CT scan data in Fig. 1(c), computer model in Fig. 4(a))
2. A replicate prototype of the nasal cavity, which is made of water-soluble cornstarch, is created by RP machine (Z Co. MA.USA). (Fig. 4(b))
3. This prototype is suspended in a rectangular Plexiglas box. (Fig. 4(c))
4. A mixture of the clear silicone and the curing agent, after vacuuming to remove bubbles, and dissolved air, is then carefully poured into the Plexiglas box through a funnel and tubing to minimize air entrainment.
5. After the silicone has been cured in an oven, the cornstarch prototype is removed with cold water.

Finally, a rectangular box containing the form of the nasal cavity can be made. (Fig. 4(d))

In this paper, with high-resolution CT scan data and the careful surface rendering in computer model and proper experimental setup, the improved nasal cavity model can be obtained. We use 166 scan data with 0.6mm scan thickness. (Somatom plus 4, Siemens. Co.) Irrelevant parts, such as sphenoid sinus etc, are carefully removed to reduce the optical noise under ENT doctor's advices. Comparing with nasal anatomy and other cavity models in Fig. 6, our cavity model has the better feature. Whereas some models are mounted improperly due to the limitation on their equipments, i.e. upside down for Hopkins' model, our model is mounted properly.

To remove the difference in the index of reflectance, the mixture of water and glycerin (52:48 in volume, $\nu = 6.55 * 10^{-6}$ m^2/sec) is used as a working fluid, as shown in Fig. 5.

Flow rate used in this study corresponds to a resting respiratory flow rate in the real nose of 125ml per sec. Since a mixture of water and glycerin (55:45 in volume, $\nu = 6.55 * 10^{-6}$ m^2/sec) is used as working fluid in PIV measurements, the Reynolds Number and the frequency parameter must be equal to those of real air breathing condition to achieve the dynamic similarity. (Scherer et al., 1989)

$$\text{Reynolds Number: } \mathrm{Re} = \frac{Ud}{\nu}, \qquad \text{Frequency Parameter: } \alpha = d\sqrt{\frac{\omega}{\nu}}$$

Where U is the average velocity in the external nares and d is the hydraulic diameter of the external nares.

Experimental Setups for PIV and the air flow resistance in breathing are given in Fig.7. A SPECTRON double pulse Nd: Yag Laser (150 mJ/pulse) is synchronized to CCD camera (LaVision FlowMaster 3, 1280 × 1024 pixel) by a Trigger Controller.

The CBC PIV algorithm with window offset (32*32 to 16*16) (Kim et al., 2001) is used for PIV flow analysis. Adjacent interrogation spots of a final stage were overlapped by 50%, providing a

resolution of 150 μm/pixel. 1024 velocity data (160*128 vectors) are averaged to give mean velocity and RMS velocity set.

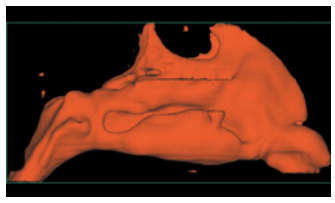

(a) Reconstructed computer image

(b) Prototype made by RP machine

(c) Model casting with clear silicon

(d) Remove box and prototype

Fig. 4. Creation procedures for nasal cavity model.

(a) Water in a flow passage

(b) Mixture in a flow passage

Fig. 5. Reflectance by working fluids.

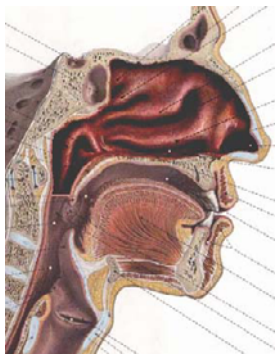

(a) Nasal anatomy (Frick et al., 1990)

(b) Scherer et al. (1989)

(c) M.M. Hess et al., (1992)

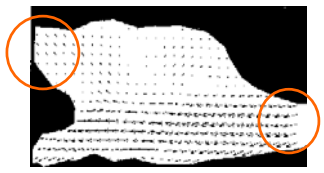

(d) Hopkins et al. (2000)

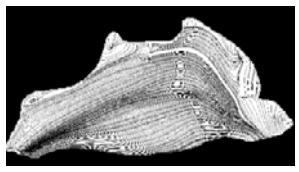

(e) S. K. Kim (2002)

Fig. 6. Comparison of various nasal cavity models: defects of each model are expressed in orange circles.

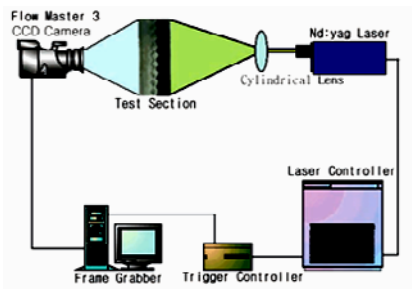

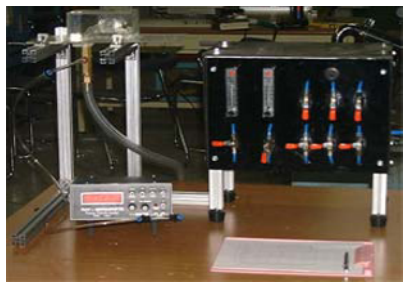

Fig. 7. Experimental set-up for PIV measurement (left) and air flow resistance (right).

4. Results and Discussion

An average velocity distribution in a flow passage near the nasal septum and concha for a normal nasal cavity are obtained from 1024 set of velocity vectors by PIV analysis, as shown in Fig. 8. Reynolds number is about 200. Larger RMS value, that is believed to be the larger heat and mess transfer, can be seen at the level of the head of the middle airway, and the flow rate was highest at the middle airway. RMS value reaches 20% of mean velocity within 3-4cm from nares that explains active heat and mass transfer as shown in Fig. 8(d).

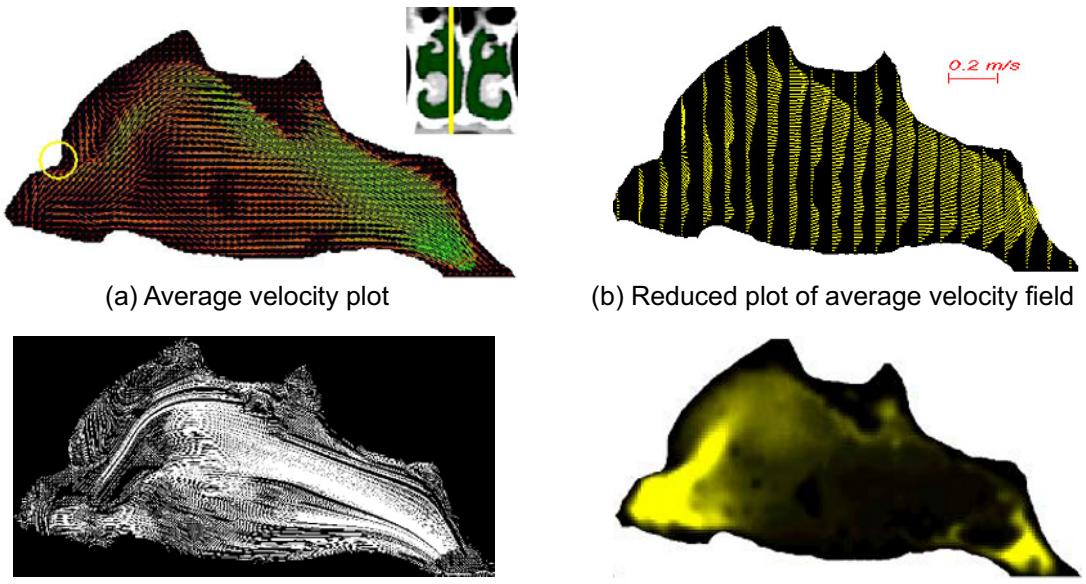

(a) Average velocity plot (b) Reduced plot of average velocity field

(c) Mean streamline (1024 images) (d) RMS distribution (1024 images)

Fig. 8. PIV results of resting inspiration (normal cavity model): Q=125ml/s and Re=200.

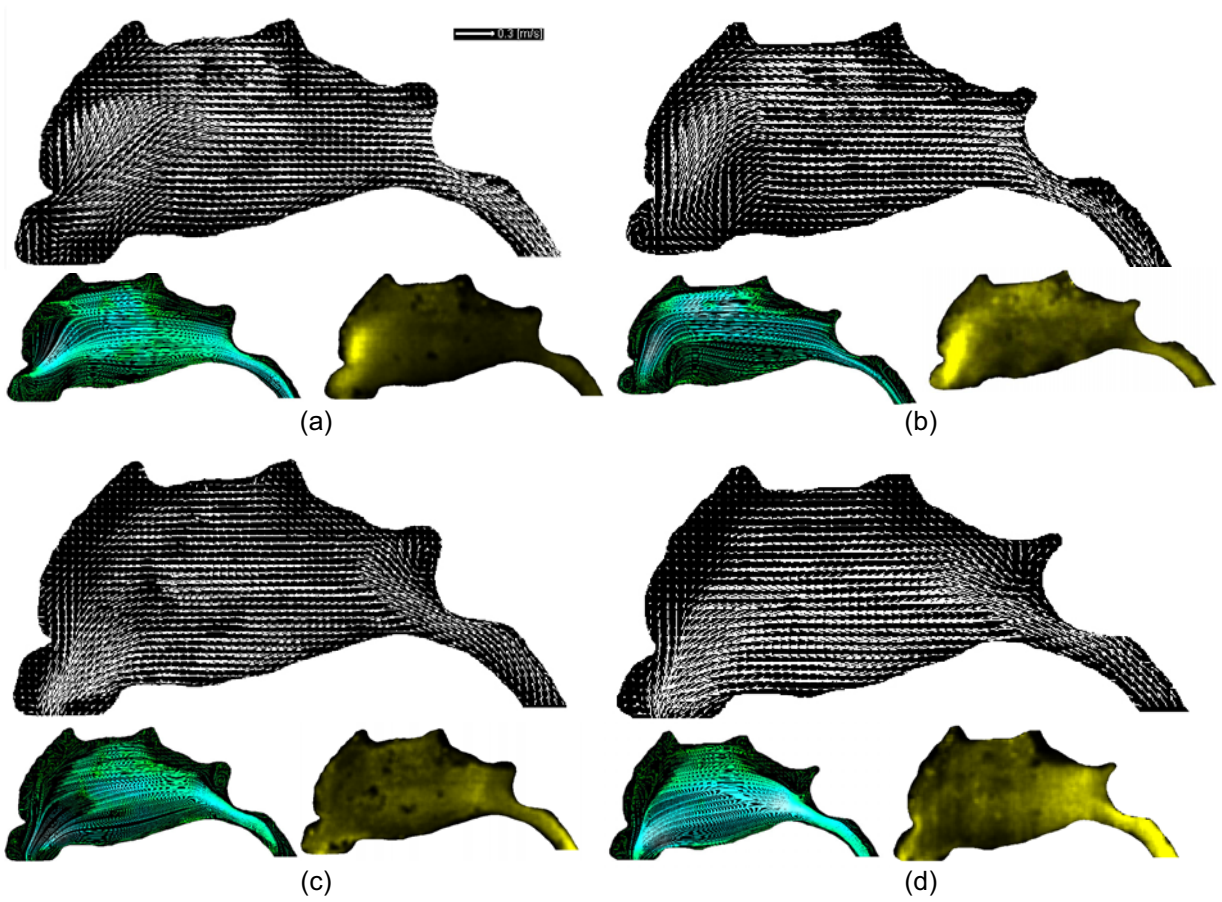

(a) (b)

(c) (d)

Fig. 9. PIV Results for adenoid vegetation (average velocity, mean streamline, RMS distribution): Q=125ml/s and Re=200 (a) 50% inspiration (b) 70% inspiration (c) 50% expiration (d) 70% expiration.

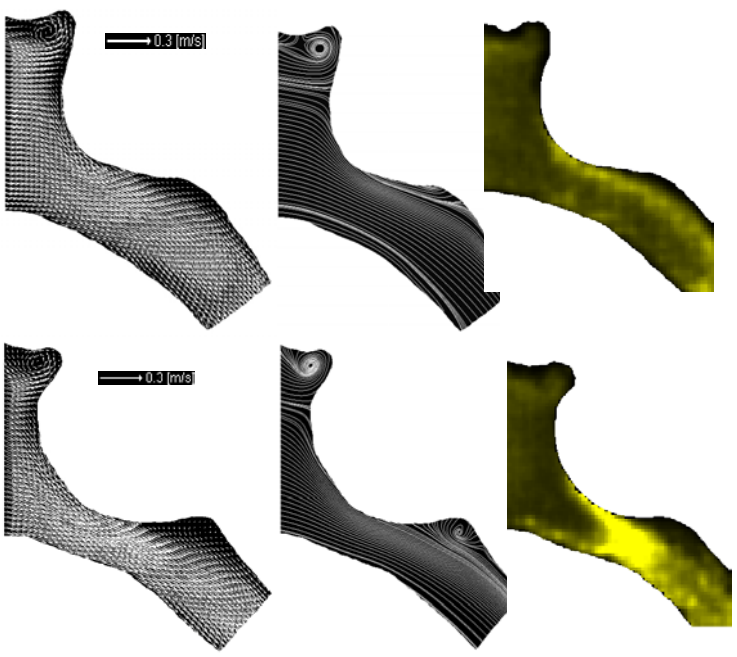

Fig. 10. PIV results of resting inspiration at throat (average velocity, streamline, RMS distribution): 50% adenoid vegetation (upper), 70% Adenoid Vegetation (lower).

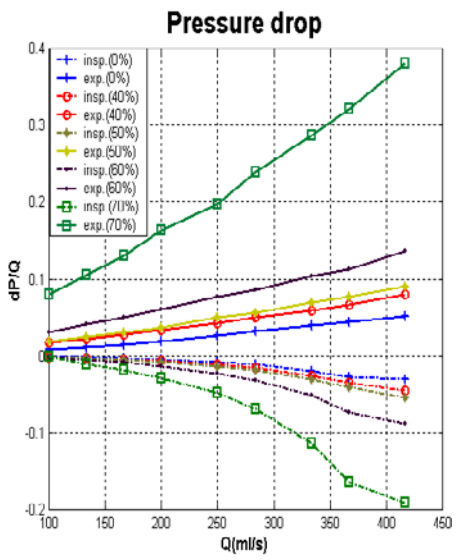

Fig. 11. Pressure drop: expiration and inspiration (lower).

The quantitative data for the cases of 50% and 70% adenoid vegetation are given in Figs. 9-11. Comparing with the normal case, the flow quantities are almost identical except the region near the upper pharynx in inspiration. But in expiration, there show some differences; growing RMS values, streamline pattern etc. In both inspiration and expiration, higher velocities and intensive concentration of higher RMS value near a swollen lymph tissue are observed, as depicted in Fig. 9. A closer look at the pharynx in inspiration, as shown in Fig. 10, leads to following conjecture; In case of 50%, blocked nose caused by excessive pressure drop is not so severe, but, in 70% case, flow resistance increases rapidly. It can be explained by flow separation and remarkable increases in RMS quantities at throat. There are two re-circulating zones in case of 70%, but there is only one in case of 50%. Actually, the decision of medical operation, made by ENT doctor, lies between 50% and 70%. It is believed that more experiments can narrow this gap. Results of pressure drop between nares and nasopharynx, that means flow resistance and depicts in Fig. 11, confirm this fact and narrow this gap between 60% and 70% in this case. The Similarity in pressure drop curves shows that flow characteristics before nasopharyns are almost identical with normal cavity case. From the linear variation of Δp with respect to Q, laminar flow persists until flow rate reaches 250 ml/sec.

One case of an asymmetric nasal cavity due to bent of nasal septum is dealt in this study. Even though the geometries of left and right cavities are quite different, as shown in Fig. 12, flow rates of

Fig. 12. Selective CT images of asymmetric nasal cavity that was used in this work.

both cavities are almost even in this case. This can be explained by the fact that this patient's nose adapts itself to this circumstance by deforming the other parts of nasal cavities. Average velocity plots and RMS distributions at various sagittal sections are shown in Figs. 13-14. Positions of each section are given at CT images in Fig. 13. Islands in Figs. 13-14 are blocked airway by swollen conchas. Local concentration of RMS values can affect not only heat and humidity transfer but also shear stress on mucosae. This concentration of shear stress may aggravate patient's condition.

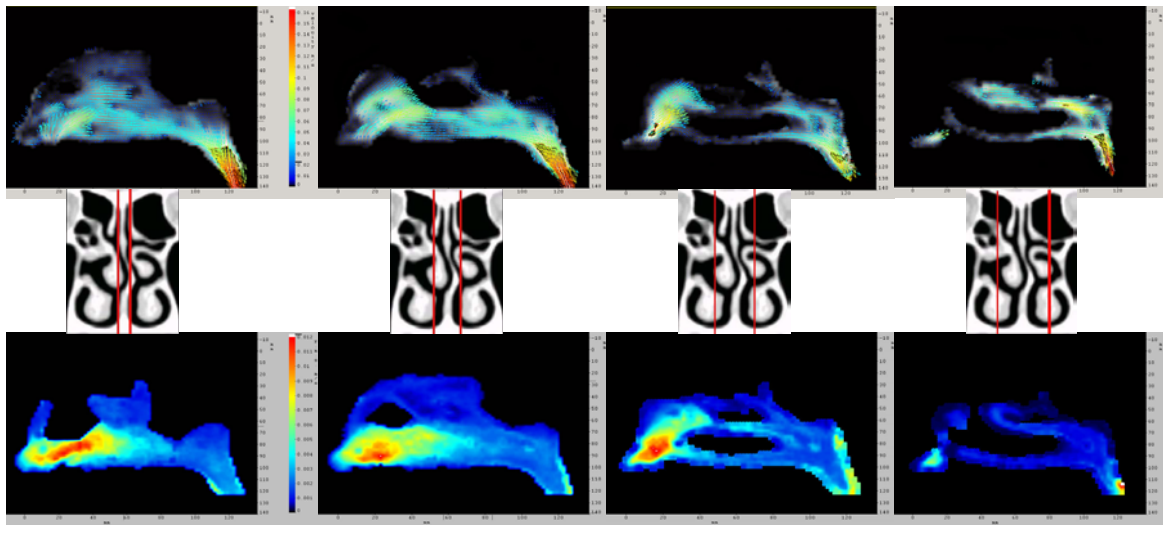

Fig. 13. PIV results of left cavity: Q=125ml/s Re=200, average velocity (upper) and RMS distribution (lower).

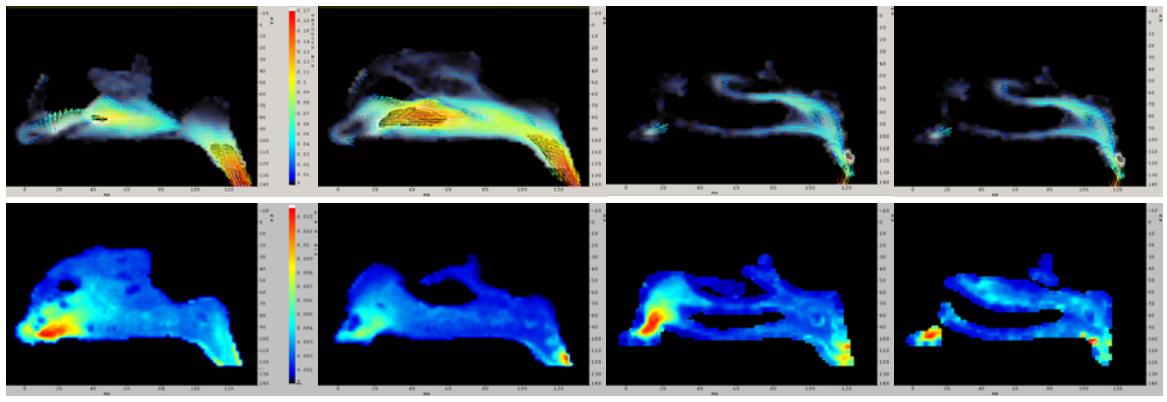

Fig. 14. PIV results of right cavity: Q=125ml/s Re=200, average velocity (upper) and RMS distribution (lower).

5. Summary

In this paper, the Procedure for flow passage with complex geometry is established. The high-resolution CT scan data and surface rendering in computer model, the improved nasal cavity model can be obtained. With this model, quantitative data for normal and pathological airways are obtained and investigated. Flow characteristics related with abnormalities in nasal cavities are conjectured in case of adenoid vegetation. The methodology in this paper can be applied to any other otorhinolaryngological diseases and contributes to help ENT doctors in diagnosis and medical treatments of these diseases.

Acknowledgement

This work was supported by Grant No. 2000-1-30400-002-3 from the Basic Research Program of the Korea Science and Engineering Foundation, Republic of Korea

References

Frick, H., Kummer, B. and Putz, R., Atlas of Human Anatomy (1990), 132, Fig.154, KARGER Co.
Hart, D.P., PIV error correction, Exp. Fluids, 29 (2000), 13-22.
Hess, M. M., Lampercht, J. and Horlitz, S., Experimentelle Untersuchung der Strombahnen in der Nasenhaupthoehle des Menschen am Nasen-Modell, Laryngo-Rhino-Otol. 71 (1992), 468-471.
Hopkins, L. M., Kelly, J. T., Wexler, A.S. and Prasad, A.K., Particle image velocimetry measurements in complex geometries, Exp. Fluids, 29 (2000), 91-95.
Kim, S. K. and Son, Y. R., An Experimental Study of Developing and Fully Developed Flows in a wavy Channel by PIV, KSME Int'l J., 15-12 (2001), 1853-1859.
Kim, S. K. and Son, Y. R., Particle Image Velocimetry Measurements in Nasal Airflow, Trans. KSME B, 26-6 (2002a), 566-569.
Kim, S. K. and Son, Y. R., An Investigation on Airflow in Abnormal Nasal Cavity with Adenoid Vegetation by PIV, Pros. ISFV10 (Kyoto), (2002b), No. J4-2-1.
Scherer, P. W., Hahn, I. I. and Mozell, M. M., The Biophysics of Nasal Airflow, Otol. Clinics N. Ame. 22 (1989-4), 265-278.

Author Profile

Sung Kyun Kim: He received his MSE in Naval Architecture in 1982 from Seoul National University. He also received his Ph.D. in Naval Architecture and Marine Engineering in 1988 from University of Michigan, Ann Arbor. He worked in Department of Mechanical Engineering, University of California, Berkeley as a visiting professor in 1997. He works in Department of Mechanical Engineering, Konkuk University, Seoul, Korea as a professor since 1988. His research interests are Flow Visualization, PIV, Biofluid Engineering, Flow Induced Vibration and Streaming Flow.

Jung Rim Haw: He received his ME in Chemical Engineering in 1977 from Seoul National University and Ph.D. in Chemical Engineering in 1984 from Polytechnic Inst. of New York. He works in Dept. Materials Chemistry and Engineering, Konkuk University, Seoul, Korea as a professor since 1985. His research interests are Rheological Behaviors of Polymers and Biomaterials.